ANFIS MPPT with power management strategy to harvest reliable power from standalone PV systems to residential loads

Subbaraman Alagammal, Ramachandran Bhavani, Mohammed Muhaidheen
Department of Electrical and Electronics Engineering, Mepco Schlenk Engineering College, Tamil Nadu, India

Article Info

ABSTRACT

In recent decades, the matching between the growing energy demand and generation is becoming the challenging task to the researcher's leads for the development of standalone solar photo voltaic (SSPV) power system. The SSPV system is more suited for electrification of essential loads uses DC power as it offers high efficiency. This work aims to model and simulate SSPV with lead acid battery is used as a DC source. The proposed series shunt charge controller with power management strategy (PMS)is designed and modeled to control the power flow among SSPV, battery and the load. adaptive neuro fuzzy inference system (ANFIS) controller effectively regulates the output voltage by controlling duty ratio of the suitable converter for driving a DC load. A PMS is developed for selecting the operating mode of SSCC by sensing and regulating the battery voltage within 11.6-12.95 V. Here, the 250 Wp panel has been employed to charge a 12 V, 34 AH battery. The practicability of SSPVB system is verified under various loaded conditions using MATLAB/Simulink for a period of 24 hours. A simulation result proves that this SSPV Battery system is capable to electrify the essential loads in rural and isolated areas and also reduce the dependency of grid power.

Corresponding Author:

Subbaraman Alagammal
Department of Electrical and Electronics Engineering, Mepco Schlenk Engineering College
Sivakasi, Tamil Nadu, India
Email: mshanthilogesh@mepcoeng.ac.in

1. INTRODUCTION

Nowadays, sustainable energy systems play a vital role for building wealthy and healthy environments. With the rise in population, the associated energy demand is also increasing tremendously in a nation. The existing system cannot meet the spurt in demand. The coastal regions and other rural areas still lack a reliable power supply. These regions use autonomous diesel generator (ADG) sets as alternative sources of power. But the ADGs are not eco-friendly. They also have high maintenance and operating costs [1]−[4]. These limitations have stimulated the scientists and researchers to look for alternate sources to produce electricity in a simple and gainful manner.

Recently, renewable energy (RE) based hybrid power generation system (HPGS) has been employed to provide power instead of DG sets in such isolated zones [5], [6]. A HPGS comprises more sources with converters and/or storage devices. In general, HPS mainly concentrate on harnessing solar and wind power. But, HPGS has some limitations like energy losses in conversion between AC and DC systems, synchronization problem, complex parameter adjustments, cost and, they are unable to match the load demand. Similarly, fuel cell can be used as energy source, but it is expensive [6]−[9].

A static fuel less solar PV system has an additional advantage of being operated in offline mode and

online mode. The online mode is more suitable for large loads in urban areas. Hence, the SSPV system which is a good choice for low and medium loads can be used in isolated areas as the main source of electricity [10], [11]. However, PV source provides different level of outputs at different instants, because the function of PV panel depends upon varying nature of insolation and temperature. Therefore, PV system has always been operated at its maximum power point (MPP). Literature illustrates that different topology of DC-DC converter with various MPPT techniques have been employed in SSPVS to obtain MPP [12]–[15]. However, such algorithms are not stable against the fast-varying environmental conditions. Hence, in this work ANFIS controller has been integrated in the SSPV system.

Furthermore, PV system power generation is intermittent and needs to store thereby it can deliver consistent power to the load. Also, to improve the reliability and competence of the SSPV system, many researchers have recommended various energy storage devices such as fuel cell, ultra-capacitor, battery banks etc. to be incorporated into SSPV system [16]–[18]. Fuel cells require hydrogen rich fuel and the voltage drop of these cells increase steeply with increase in load. They also face the possibility of fuel starvation. These factors decrease the lifetime of the fuel cells [19], [20]. Ultra-capacitors are rapid charging and discharging devices, but they are expensive.

Batteries have beneficial features such as wide operating temperature range, less discharge, long lifetime and low fixing cost [21]. Taking the above points into consideration, it is an excellent choice to use batteries as a sink or as a back-up source in small or medium sized SSPVs for making the system to be an efficient and successful. However, the lifetime of battery gets reduced if there is an uncertainty in input or improper charging and discharging for long period. In addition, batteries are more related for most failures occur in PV system. To overcome the above-mentioned concerns, battery charge controllers must be integrated in solar system. Its sole purpose is to protect the battery from being overcharged or over discharged and also supports to extend the battery life.

Based on recent reviews, a conventional bidirectional converter has been used as a charge controller (CC) for correcting the battery output. But it leads to complexity in design and more switching losses [20]. Some good works based on a shunt or series charge controller has already existed, but it uses more switches individually to control the operation of batteries fed from any source. Moreover, shunt controllers are limited to use for high current and need heat sink for power dissipation [21], [22].

In this paper, a combined series shunt charge controller (SSCC)with preset voltage control using electronic switching technique has been employed so that the number of switches used gets reduced. In addition, the voltage control loop process gets simplified. Besides, to improve the battery performance, an adequate knowledge of battery output and SOC is required which become the motivation of this research [23]–[25]. Hence, battery voltage and SOC can be maintained within a preset limit because SOC is directly proportional to terminal voltage of battery. Also, it is more efficient because the issues related to series, shunt or bidirectional converter CC can be eliminated.

The main objective of this proposed work is to model a new configuration of CC along with ANFIS MPPT control algorithm to obtain the desired output for regulating the power among the sources and the loads by considering 8.64 Ω resistors as a constant and variable DC loads from an emerging APVB system. Also, the system has been examined by evaluating and comparing the performance of the proposed CC in terms of SOC and terminal voltage (12V) of battery for 24 hours with respect to various levels of insulation. The feasibility of the projected APVB structure is to realize the good voltage regulation and maximum power extraction for upgrading solar conversion efficiency and the extend the battery life with a view to get desired power for DC loads.

2.   PROPOSED SYSTEM DESCRIPTION

The block diagram of SSCC fed battery integrated SSPVG System is shown in Figure 1. In order to supply uninterruptable power to the residential loads affordably, battery backup unit with a suitable charge controller is implemented. In this study, the bidirectional power flow of battery with the rest of the system occurs through SSCC employing a simple logic control electronic switching PMS instead of bidirectional converter which is suitable for the compensation of source power and demand power. Further, it can be used to prevent the reverse current flow to PV panel during night, low PV power and less loaded conditions thereby improving the performance of module.

2.1.   System modeling and description
2.1.1. Modeling of SSPVG

The SSPVG consists of a PV array, a buck-boost converter and an MPPT controller. A BB converter is used to obtain the desired output from the PV array using ANFIS MPPT through the adjustment of duty ratio. The SSCC is capable of operating in both series and shunt modes to regulate the battery output voltage [10]. The relationship between the powers of various elements in solar system is given by (1).

$$P_{out}(t) = P_g(t) + P_L(t) \tag{1}$$

where $P_{out}(t)$ is the instantaneous output power of the BB converter in SSPVG, $P_B(t)$ is the power delivered by the battery and $P_L(t)$ is the power consumed by the dc load. The variations in PV power due to the change in solar radiation and the load power cause deviation in the battery voltage and converter output voltage.

$$V_{out}^2(t) - V_{or}^r(t) - 2tP_g(t) = P_{out}(t) - P_L(t) \tag{2}$$

From the above equation, it is inferred that the power transfer among the source, battery and load depends on the difference in instantaneous converter output $V_{out}(t)$ and instantaneous reference voltage $V_{or}(t)$.

Generally, the traditional BB converter provides negative output which is not suited for many applications. Figure 2 shows the proposed BB converter provides the positive output for any value of duty cycle. Moreover, it has only two switches operating in continuous current mode and also provides ripple less current in the output inductor. The converter is found to be stable with positive output voltage and no zeros in the right half of s plane. Here, the converter is employed in closed loop to provide a required voltage for battery charging and the load [11], [12].
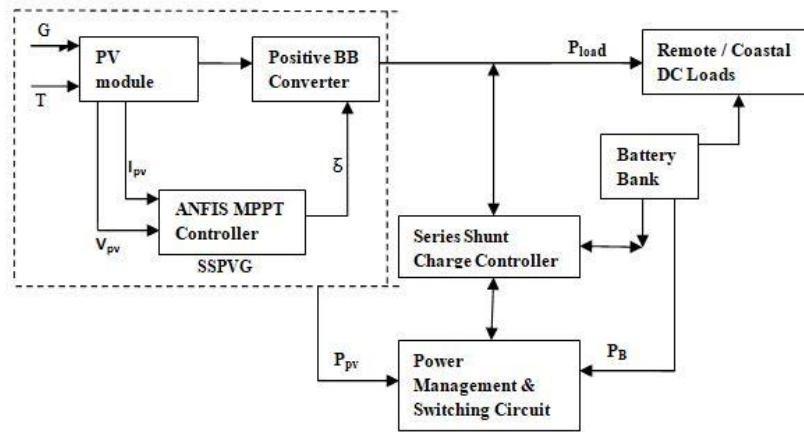

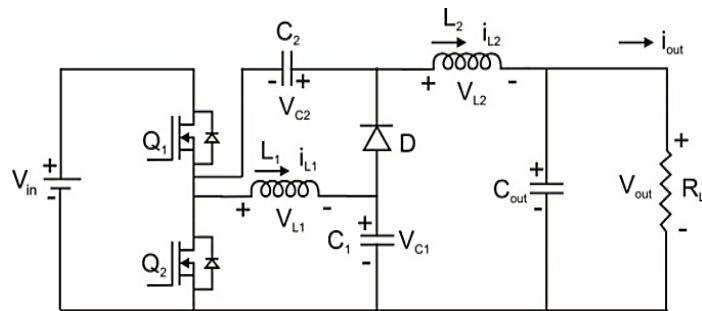Figure 1. Block diagram of the proposed SSCC integrated PV – battery system

Figure 2. Circuit configuration of dual mode positive output buck boost converter

The voltage gain is elevated in both buck and boost operating modes with reduced losses with same input voltage polarity. In buck mode, the switch Q_2 is never being turned on and the regulated output voltage is obtained by the first switch Q_1 in the continuous current mode. Whereas in boost mode, the first switch Q_1 is always short circuited and the diode is open circuited and the regulated output voltage is obtained by switching Q_2 of the converter. If V_{pv} and I_{pv} are the PV voltage and current fed as an input to the BB converter working at a duty cycle δ, the voltage transfer gain can be written as in (3)

$$\frac{V_{out}(t)}{V_{in}(t)} = 2\delta \tag{3}$$

2.1.2. Control strategy of ANFIS MPPT

An ANFIS is a kind of intelligent network that is based on Takagi–Sugeno fuzzy inference system (FIS) [13]. The data used in ANFIS controller for training was obtained from the PV panel output. The input variables of ANFIS controller include error E(k), and the change in error ΔE(k) as given in (5)-(6) and the output is duty cycle δ. Here:

$$V_{in}(k) = V_{ref}(k) = V_m(k) \tag{4}$$

$$E(k) = V_{in}(k) - V_{pp}(k) \tag{5}$$

$$\Delta E(k) = E(k) - E(k-1) \tag{6}$$

A gradient-based learning procedure is usedfor updating these parameters according to given training data to attain a desired input-output mapping. Their control strategy is defined under different cases and the corresponding block diagram is shown in Figure 3. Where V_m (k)-maximum voltage or reference voltage, V_{pv} (k)-instantaneous PV output voltage and V_{pv}(k-1)-PV output voltage at the previous instant (k-1).
- Case 1: E (k) =0

$$V_{pv}(k) = V_{pv}(k-1) = V_m(k) \tag{7}$$

It implies that the instantaneous output voltage of PV source reached the Maximum Operating Point (MPP) value hence error is zero.
- Case 2: E (k) = +ve

$$V_{pv}(k) > V_{pv}(k-1) \tag{8}$$

This states that the instantaneous output voltage of PV panel goes beyond the maximum value which depicts that the error becomes positive. So, the controller adjusts the duty cycle to decrease thereby brings V_{pv} (k) to the V_m (k).
- Case 3: E (k) = -ve

$$V_{pv}(k) < V_{pv}(k-1) \tag{9}$$

This depicts that the instantaneous output voltage of PV panel goes below the maximum value so that the controller adjusts the duty cycle to increase thereby brings the operating point to MPP ie V_m (k).
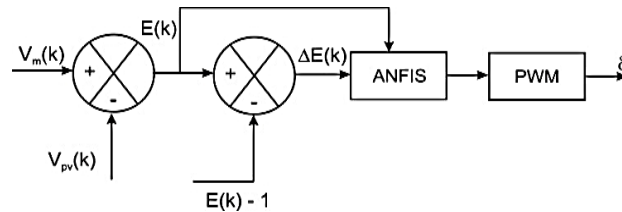

Figure 3. Control block diagram of ANFIS MPPT controller

Table 1 clearly specifies the setting of essential parameters for modeling of ANFIS network. Fuzzy subsets for the inputs to the ANFIS controller are expressed by using 8 variables with gaussian membership functions (GMF). An error E (k) containing the range of values (-5, 5), and the range of change in error values ΔE (k) (-1, 1) and step size will be 0.5 as the trained data. Hybrid Back propagation learning algorithm is worked to control the parameter of membership function. GMF is specified by three parameters such as mean, sigma and normalization. Therefore, the ANFIS used here contains a total of 224fitting parameters, among these $32((8 \times 2) + (8 \times 2) = 32)$ are the argument parameters and $192(3 \times 64 = 192)$ are the subsequent parameters.

Figure 4(a) shows the structure of TS FIS based ANFIS network. The training and testing root mean square (RMS) errors obtained from the simulated ANFIS are 0.006 and 0.076 respectively as shown in Figure 4(b). It is clear that the disturbances in dc voltage are revealing in the PV power and move the PV power from the MPP until the dc voltage has been regained. Hence, rapid regulation of dc voltage is essential

to maintain a constant dc voltage. For that, a charge controller is proposed to regulate the battery voltage in order to provide a constant input voltage to the DC loads.

Table 1. Parameter setting for ANFIS modeling

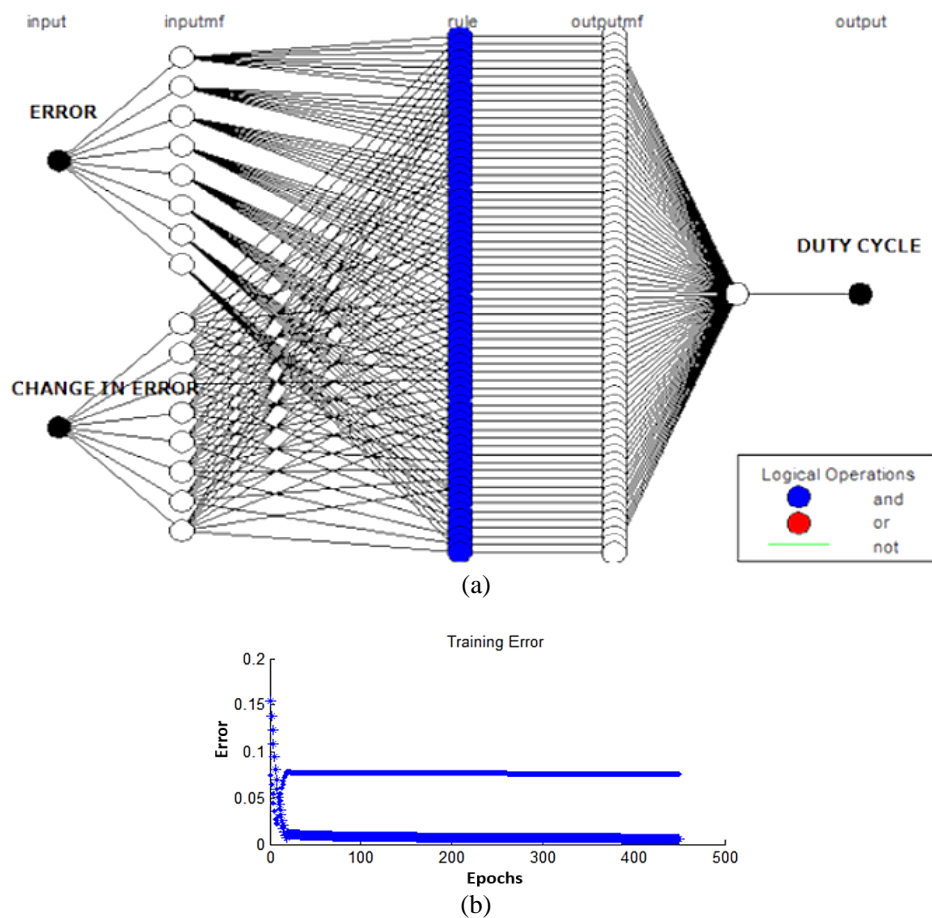| Parameters	Values
Membership function	Gaussian
Fuzzy inference system	Takagi-Sugeno
Number of epochs	450
Number of input membership functions	8 each
Number of rules	64
Types of MFs	Gaussian
Fitting parameters	224
Premise parameters	32
Consequent parameters	192
Root mean square error under training	6e-3
Root mean square error under testing	7.6e-2

(a)

(b)

Figure 4. Simulink model of controller and its output (a) ANFIS structure, and (b) error vs epochs

2.2. Battery modeling

Generally, SSPV unit needs to satisfy the load demand all the time without any interruption. In this work, a Lead Acid Battery (LAB) has integrated with generation system for enhancing the reliability of the system. The rated specifications of LAB are given in Table 2. The role of the LAB bank is to accumulate the excess power from SSPVG unit thereby compensating for the mismatches between the source and load. To analyze the performance of LAB, it is needed to develop the model based on typical equivalent circuit as shown in Figure 5 using MATLAB/Simulink environment [19]–[25].

Also, the State of Charge (SOC in %) is directly proportional to the open-circuit terminal voltage (V_{bat}) of the battery. Hence, based on preset battery voltage and SOC bounded limit the battery can be

operated in two modes like charging and discharging. The equations (10) to (15) define identifying the modes of operation of the battery. The implementation of the model of ns cells in series implies necessarily assigning dissimilar expressions to the values of V_1 and R_1 in each mode. SOC (t) can be computed based on the present open-circuit terminal voltage of the battery in both modes of operation.

Table 2. Parameter specifications of lead acid battery

Parameters	Values
Nominal voltage	12 V
Nominal capacity	40 Ah
Nominal temperature	-27°C

Charge mode: By applying KVL to the equivalent circuit, the instantaneous value of the terminal voltage V_{bat} of the battery is given as.

$$V_{bat} = V_1 + I_{bat}R_1 \tag{10}$$

The electromotive force V_1 and the internal resistor R_1 are functions of the internal components of the battery are given by the following equations.

$$V_1 = V_{ch} = [2 + 0.148 \times soc\,(t)] \times n_s \tag{11}$$

$$R_1 = R_{ch} = \frac{0.758 + \frac{0.1309}{1.06 - soc(t)}}{soc_m} \times n_s \tag{12}$$

Discharge mode: The mathematical expressions are similar to those found at charging mode with a sort of variation concerning the values.

$$V_1 = V_{dch} = [1.926 + 0.124 \times soc(t)] \times n_s \tag{13}$$

$$R_1 = R_{dch} = \frac{0.19 + \frac{0.1037}{[soc(t) - 0.14]}}{soc_m} \times n_s \tag{14}$$

$$V_{bat} = V_1 = I_{bat}R_1 \tag{15}$$

The parameters used are I_{bat} – terminal or instantaneous values of battery current, SOC(t) – instantaneous values of state of charge, SOC_m – maximum value of state of charge and n_s – number of cells in series.
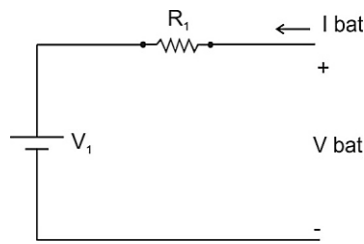

Figure 5. Equivalent circuit of battery

2.3. Series shunt charge controller

In this work, a new topology of SSCC as shown in Figure 6 has been proposed to control the battery operation by acquiring the gain of both series as well as shunt controller. The series controller of switch SA on the PV module side gets turned off if the battery voltage becomes larger than 12.95 V and will remain open until the battery voltage has dropped to 12.2 V. The switch SB on the load side called shunt or load controller is opened if the battery voltage drops below 11.6 V and will remain in that state until the voltage has been recharged to 12.25 V.

The switch SC supplies the PV power to the load directly whenever the PV power equals the load power. The function of switches SC and SD are used to draw away an extra current from the SSPVG module to the dummy load when the battery is fully charged. There is a reverse blocking diode D that only allows

positive current and also prevents the SSPVG from reverse battery power when the insolation level is low. Finally, the duty cycle is also found in this block by passing the ratio of battery voltage to PV module voltage through the (u/(u+1)) block. The switching control strategy of SSCC is implemented using MATLAB Simulink. The SSCC commands the battery to deliver power to load when there is no adequate PV power and to charge when surplus PV power is obtained. Thus, the voltage control loop of the SSCC circuit decides the operating mode of the battery.
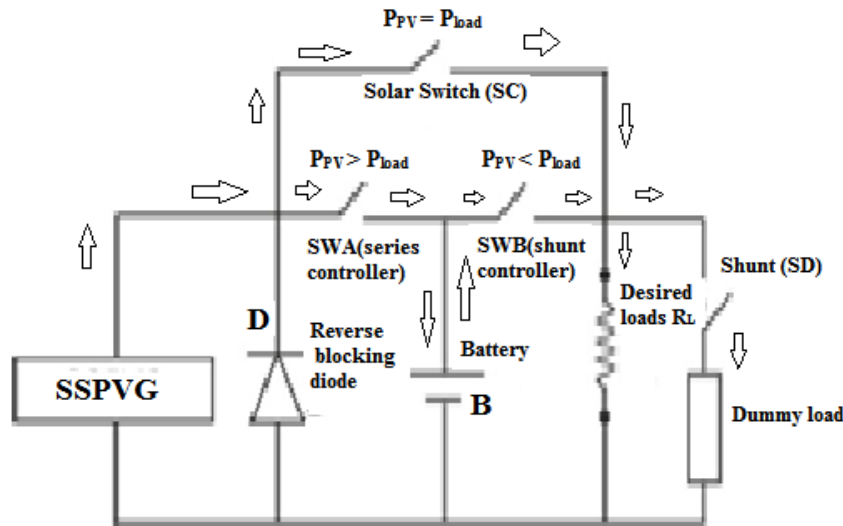

Figure 6. Proposed SSCC for solar system

2.4. Power management scheme (PMS)

The PMS operates under preset voltage control mode (PVCM) in order to manage the power flow among PV panel, battery and load in a solar system. The PMS continuously monitors the battery voltage, PV power and demand power accordingly a control signal is generated for controlling the on – off operation of switches used thereby deciding the operating modes of CC as shown in Figure 7. The typical power balance equation of the proposed system is given as.

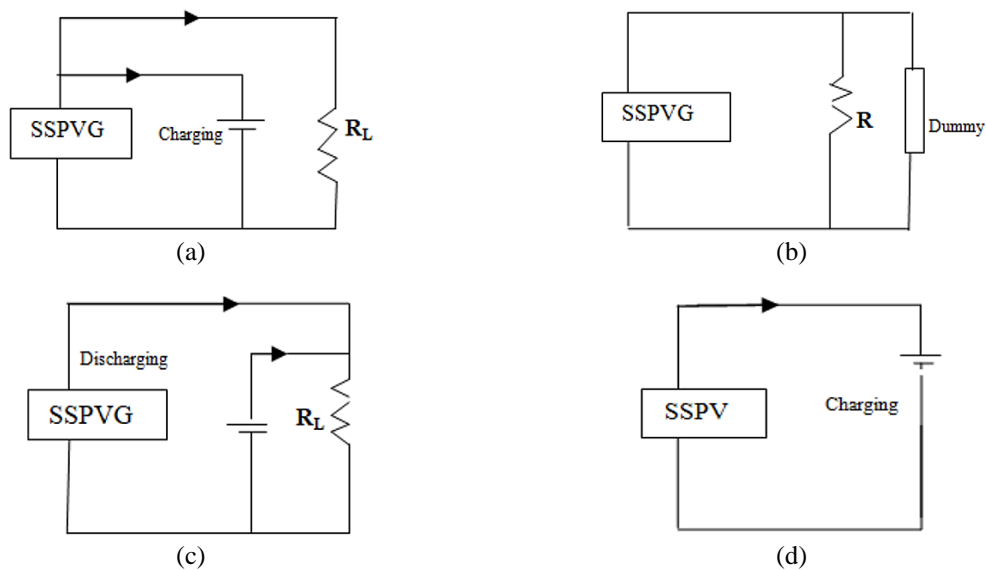$$P_{pv} + P_{bat} = P_{load} \qquad (16)$$

Figure 7. Equivalent circuit (a) mode1, (b) mode 2, (c) mode 3, and (d) mode 4

2.5. Logical switching modes of operation

The description of equivalent circuit of all the modes is explained in this section.

− Mode 1: $P_{pv} > P_{load}$ and $V_{bat} < HVD$ (12.95 V)

The generated power is greater than the load demand. So, the excess power can be used to charge the battery when the battery has a voltage less than the HVD. Here the switch SC closes connecting the SSPVG to the load. In addition, SA is also closed causing the battery to enter the charging mode. The switches connecting the battery to load (SB) and the dummy load (SD) remain open. There is no discharge of battery power.

− Mode 2: $P_{pv} > P_{load}$ and $V_{bat} > HVD$ (12.95 V)

Again, the generated power is greater than the load demand. However, the battery cannot be charged further as it has already reached the HVD limit. The battery can be further charged only after the battery voltage has dropped to LVR (12.2 V). Therefore, the switch SA is opened. Normal operation of the load under the SSPVG power takes place by SC is closed. Then, the excess SSPVG power is diverted to the dummy load by closing the switch SD. The battery is isolated as switch SB is also open since there is no need for battery power.

− Mode 3: $P_{pv} < P_{load}$ and $V_{bat} > LVD$ (11.6 V)

The power generated in the SSPVG is not sufficient to meet the load demand. Therefore, the battery power has to be taken into consideration. If the battery voltage is greater than the low voltage disconnects limit of 11.6 V, then the battery can be connected to the load in the discharge mode. Switch SB that connects the battery to the load is closed while the switch SA remains open. The dummy load is also disconnected from the circuit by opening the switch SD. SSPVG provides a part of the load demand by the closure of switch SC.

− Mode 4: $P_{pv} < P_{load}$ and $V_{bat} < LVD$ (11.6 V)

In this case, the power generated by the SSPVG is not sufficient to meet the load demand and the voltage in the battery is below the LVD which means it cannot be connected in discharge mode. Therefore, the switches SC, SB and SD are opened isolating the load and dummy load from the system. Switch SA is alone closed.

Thus, the power from the SSPVG is used to charge the battery. Once the battery voltage exceeds the High Voltage reconnect (HVR) value of 12.25 V, the switch SA opens while switch SB and switch SC close making the system operate in Mode 3. The power management control strategy for the entire SSPVG system using SSCC based on Preset Voltage of battery is illustrated in Table 3.

Table 3. Power management control strategy for the overall standalone SSPVG system using SSCC based on preset voltage of battery

Mode	P_{pv} and P_{load}(W)	V_{bat}(V)	SA	SB	SC (Solar switch)	SD (Shunt)	Load – status	Battery-status	Limit of V_{bat}	Next possible mode
1.	$P_{pv} > P_{load}$	Less than HVD	1	0	1	0	Connected to PV	Charging	Till HVD	2 or 3
2.	$P_{pv} > P_{load}$	Greater than HVD	0	0	1	1	Connected to PV	Isolated	Till LVR	3
3.	$P_{pv} < P_{load}$	Greater than LVD	0	1	1	0	Connected to PV and battery	Discharging	Till LVD	4 or 1
4.	$P_{pv} < P_{load}$	Less than LVD	1	0	0	0	Isolated	Charging	Till HVR	3 or 1

Figure 8 represents the flow diagram of the energy or power management strategy for the proposed SSPV system. The solar PV is considered as the main source of the system. The deviation between the generation power and the load demand is considered. In view of that, the battery unit is operated to provide reliable power to loads.

Here, V_{bat} – battery voltage, P_{pv} – power produced by SSPVG, P_{load} – power demand by load, HVD–high voltage disconnect (12.95 V), LVD –low voltage disconnect (11.6 V), LVR – low voltage reconnect (12.2 V), HVR – high voltage reconnect (12.25 V), 1 – switch is closed, 0 – switch is opened.

2.6. Load profile

The first and foremost effective way to meet the demand is achieved by collecting information regarding future load requirements in order to expand the generation by sustainable energy sources. Therefore, load management plays a vital role in estimating or designing the source requirements for the future. Based on load profile with time scale, operational decisions can be made efficiently. A real investigation was done on the electricity consumption in the village of Amathur (Sivakasi, Tamil Nadu) for a set

of houses on a daily basis. Electrical loads are assumed according to the demand data collected from the set of houses in person. The frequently used electrical devices like lamps, fans, televisions and radios are mostly run on AC right now. These are being considered as DC based load is used to build this model. According to the managerial strategy, the loads used in the habitat were further divided into two types, as follows:

2.6.1. Constant load

To begin with, a single resistor is used to represent lamp load (pooja rooms) as a constant load. The total energy demand is found by considering it to be 400 Wh/day. At 12 V and keeping the load constant over a full day (24 hours), the resistance was found to be 8.64 Ω as shown in Table 4. This table clearly depicts the representation of energy allocated to the considered load in terms of power and its operating time.
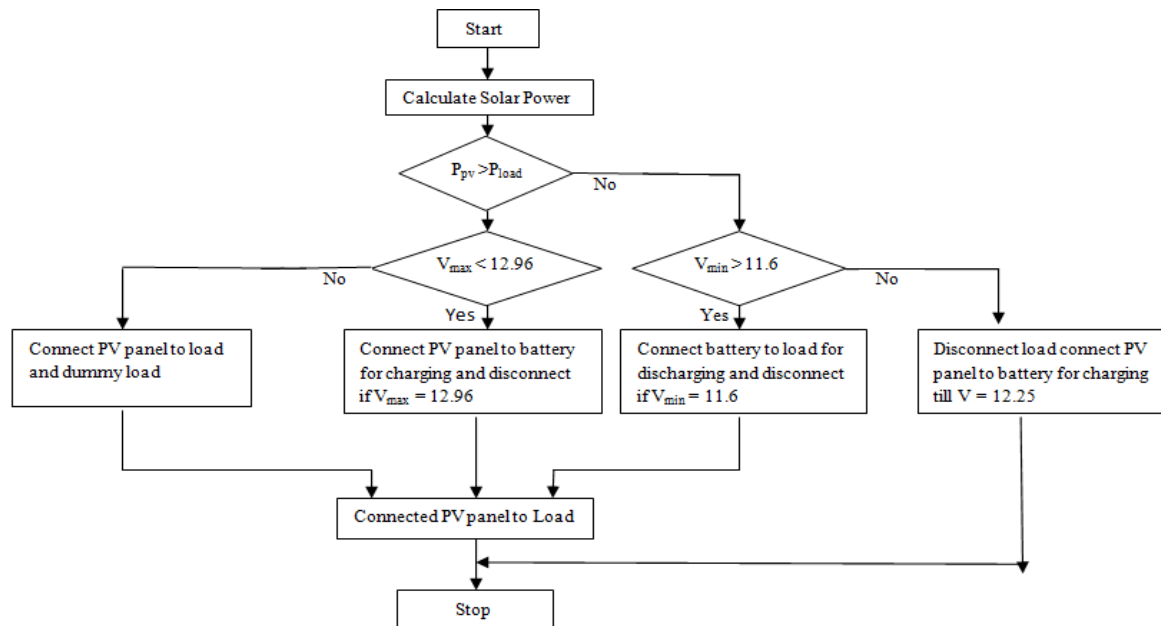

Figure 8. Power management strategy for overall PV system based on preset voltage band of battery

Table 4. Energy allocation for constant load

Load description	Voltage (V)	Power (W)	Current (A)	Time (hr)	Resistance (Ω)
Constant load	12	16.67	1.39	24	8.64
		Total energy use allocation	400 Wh / 34 Ah		

2.6.2. Various loads

The loads used to process the load management are computer/communication devices, pump/motor, Portable battery charging, and lighting. At 12 V and by varying the current usage over a full day (24 hours), the resistances are found to be of different value as given in Table 5. This table clearly depicts the representation of energy allocated to various kinds of loads in terms of power and its operating time.

Table 5. Energy allocation for various loads

Load description	Current(A)	Power (W)	Operating time (hour)	Resistance (Ω)
Lighting (load 1)	1.26	15	4	9.6
Pump/motor(load2)	15.61	187	1	0.77
Computer/communication devices (load 3)	4.18	50	2	2.88
Portable battery charging(load)	0.88	10	5	14.4
Total energy use allocation 397 Wh / 34 Ah / 12 V				

2.6.3. Design/estimation of PV system

To design the SSPV energy system, it is necessary to know the total power of the loads to be connected to the system and thus, determine the daily energy that will be needed for the station. The calculation of the theoretical energy required per day is estimated by:

$$E_{Tot} = \sum_{i=1}^{n} W_i x h \tag{17}$$

where E_{Tot} – total energy required (Wh), h – load usage time (hours), and W_i – rated load power (watts).

From this value, the actual energy consumption must be calculated by considering the various loss factors in the PV system based on the following equation:

$$E_{TR} = \frac{E_{Tot}}{P_a} = \frac{400}{0.809} = 449 \, wh \tag{18}$$

here, E_{TR} is the actual energy (Wh), P_a = Global performance of PV system = 0.809.

To estimate the capacity of the storage system, it is necessary to calculate the number of days that the system is able to operate even under no sunlight and the maximum discharge rate (DOD) that the battery can reach. For this, in (4) is used.

$$B_{cap} = \frac{E_{TR} \times 3}{V_{pv} \times DOD} = 37.5 \, Ah \tag{19}$$

Lastly, after determining the battery's capacity, the number of batteries that will be connected in parallel is defined to have a bank of batteries, so that it is able to provide back up to the system for the required days of autonomy. The number of batteries (N_{bat}) required is determined by:

$$N_{bat} = \frac{C_B}{C_F} = 1 \tag{20}$$

where C_B – actual battery capacity required is 37.5 (Ah) and C_F – battery capacity specified by the manufacturer is 40 (Ah) and hence one battery bank is required for the system for an actual total capacity of 37.5 Ah.

3. SIMULATION MODELING

To evaluate the performance of the proposed system with developed control strategy, the time-domain simulation studies in MATLAB/Simulink environment are presented. The system consists of a PV panel, a buck-boost converter, SSCC circuit for the battery and load. The details of the specifications of different elements are shown in Table 6. A BB converter raises or lowers the PV voltage based on load demand. The SSCC is built with four switches using power insulated gate bipolar transistor (IGBT) and the gate pulses to the switches are fed through pulse generator circuits. A SSCC which can operate in either series or shunt mode acts as the charger/discharger circuit of the battery. The well-known logic control electronic switching technique [25] is used to control the SSCC circuit. The voltage control loop of the SSCC circuit maintains the battery voltage at 12 V. The control algorithm including MPP tracking, dc voltage control and the power management system are implemented in MATLAB/Simulink. The performance of solar system integrated with battery charge controller under constant load and variable load conditions for a step change in insolation is analyzed [22]–[25]. The control strategy of the PMS is verified for different modes of operation under various loaded conditions.

Table 6. Design values of PV module, Positive output BB converter

PV Module at STC		Positive output BB converter	
Parameters	Ratings	Parameters	Ratings
Voltage at P_{max} (V_m)	36.84 V	DC input voltage	10 V – 16 V
Current at P_{max} (I_m)	6.86 A	DC output voltage	12 V
Maximum Power (P_m)	252.54 W	Capacitor (C_1)	> 150e-6F
No. of cells in series (N_s)	48	Capacitor (C_2)	> 150e-6F
Shunt resistance (R_{sh})	220.19 Ω	Rated DC load current	3 A
Series resistance (R_s)	0.64 Ω	Switching frequency	200 KHz
Short circuit current (I_{sc})	7.28 A	Inductor (L_1)	> 12.5e-6H
Open circuit voltage (V_{oc})	44.92 V	Inductor (L_2)	> 12.5e-6H

The Simulink model of the SSPVG system with ANFIS MPPT and charge controller and loads are shown in Figure 9. The modeling of proposed ANFIS MPPT where the E(k) and ΔE(k) are the input and generate the signal for the switches in the proposed KY–SR BB converter for absorbing the high power from PV is done. Here, the battery charger SSCC has been used to regulate the charging and discharging of battery thereby it extends the battery life by maintaining the constant voltage at 12 V. Figure 10 emphasize the modeling of proposed power flow management scheme through CC where the PV voltage, PV current and

battery voltage are the input and generate the signal for the switches in the proposed SSCC for distributing the reliable power to the load. The battery is in charge mode when the current into the battery is positive, and discharge mode when the current is negative.
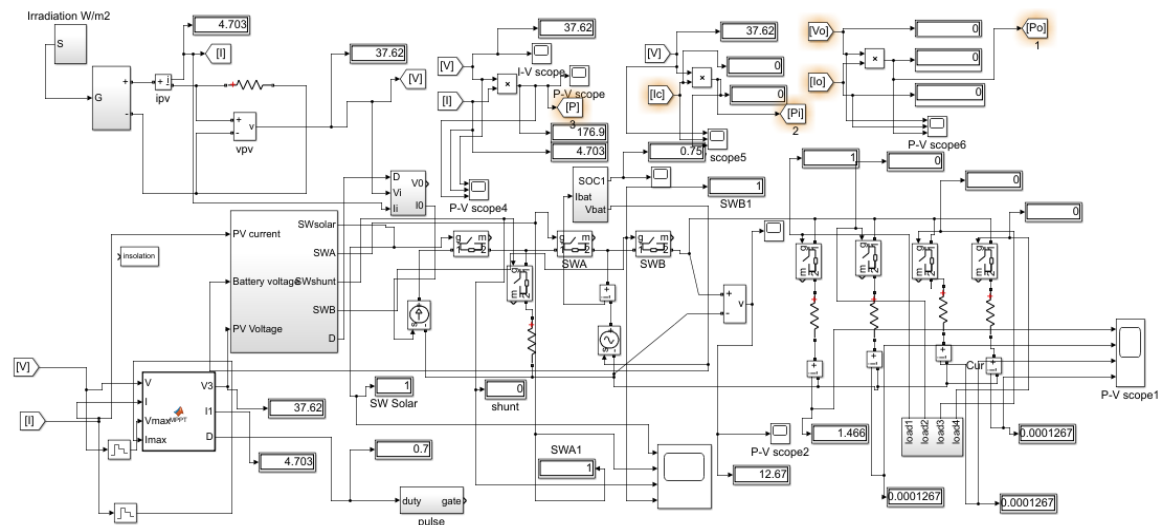

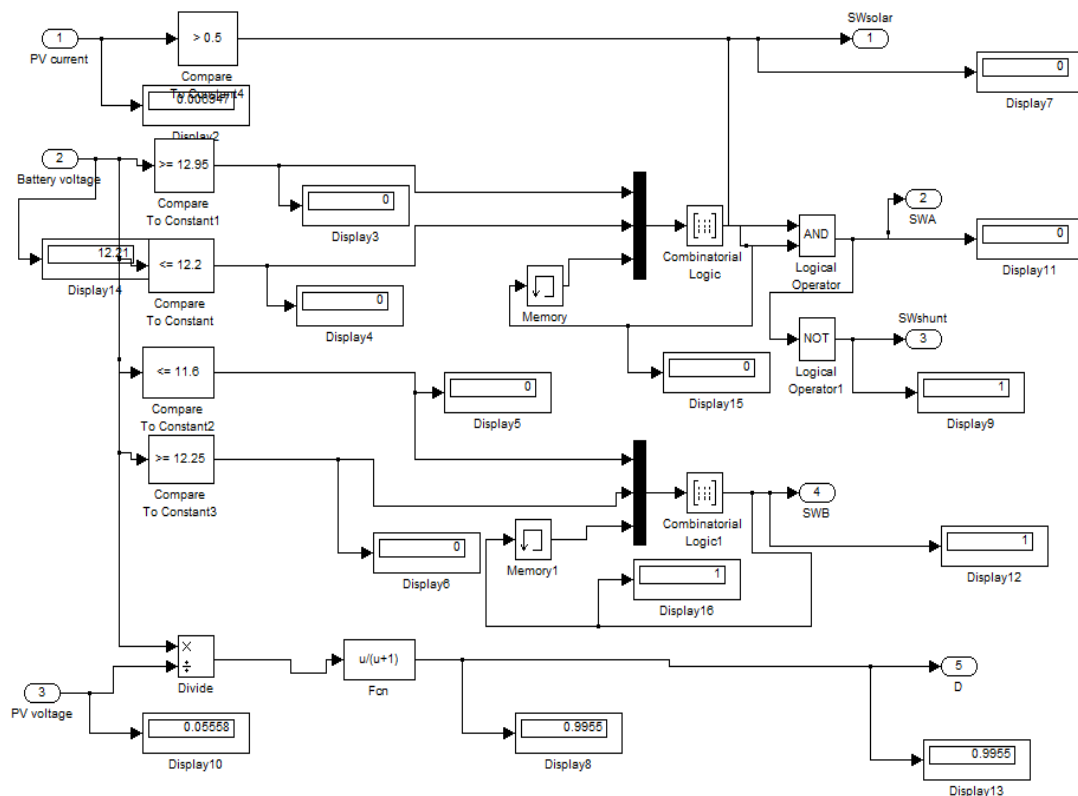Figure 9. Standalone solar PV battery system with all controllers (ANFIS MPPT and charge) and loads

Figure 10. Simulation diagram of proposed power management scheme

4. RESULTS AND DISCUSSIONS

To validate the functioning of the system, simulation studies have been carried out using practical load demand data. A real investigation was done on the electricity consumption in the village of Amathur

(Sivakasi, Tamil Nadu) for a set of houses on a daily basis in person. In this work, these are being considered as DC loads. The loads used to model the load profile are computer/communication devices, pump/motor, Portable battery charging, and lighting as resistors in simulation. For analysis, the loads used in the habitat were further divided into two types such as constant load and variable load as follows:

4.1. Constant load analysis

To begin with, a single resistor is used to represent lamp load (pooja rooms) as a constant load and the total energy consumption per day is calculated and the corresponding waveforms of different insolation levels are given below. At 12V and keeping the load constant over a full day (24 hours), the resistance was found to be 8.64Ω. Figure 11(a) shows the PV output of voltage, current and power waveforms during different insolation level W/m² varies from 100, 200, 300, 1000, 800 and 0.01 under constant load condition. Figure 11(b) shows the respective output voltage of converter for the PV input increases stepwise based on time and the level of insolation.
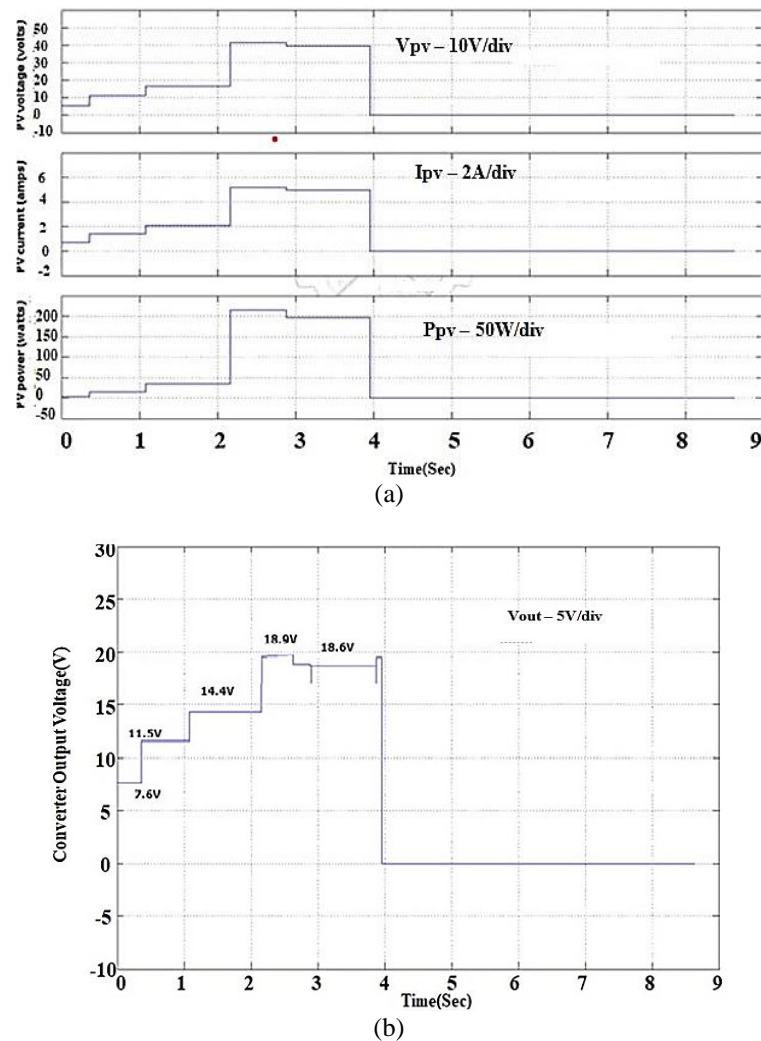

(a)

(b)

Figure 11. Output of PV source and converter for a step change in Insolation level at constant load: (a) PV voltage, current and power waveforms and (b) converter output voltage waveform V_{out} – 5 V/div

In order to see the effectiveness of using a battery, the ON-OFF status of the proposed SSCC was studied under two scenarios. The ON-OFF status of switches used in SSCC is shown in Figure 12(a). From the Figure 12(a), it is clear that, the shunt (SD) switch alone remains open to prevent the current reversal of battery and the other switches are on to do charging and also connect the load to the SSPVG. After a certain period, the switch SA gets opened to prevent the battery from getting overcharged and the shunt (SD) gets turned on to absorb the excess power. In the next period, solar switch (SC) also gets opened when the sun is

down and also switch SA remains open implies that, no charging occurs. During the last period, the battery alone supplies the power to the load through Switch SB. Three status of the battery are observed from Figure 12(b). respectively, +ve for charging, -ve for discharging, and 0 for floating during the simulation. From the Figure 12(b), it was observed that, the negative battery current clearly depicts that the battery is getting discharged and the battery current.

From the Figure 13(a) and Figure 13(b), it was inferred that the total Ampere hour is equal to 34 Ah ($1.39 \times 24 = 34$ Ah) and the energy consumed by the load is found to be ($16.67 \times 24 = 400$ Wh) equal to 400 Wh/day. The total energy demand is found by considering it to be 400 Wh/day. The proposed system includes battery charger with PMS using logical control electronic switching shows a maximum SOC of 92.13% at 12 AM as shown in Table 7.
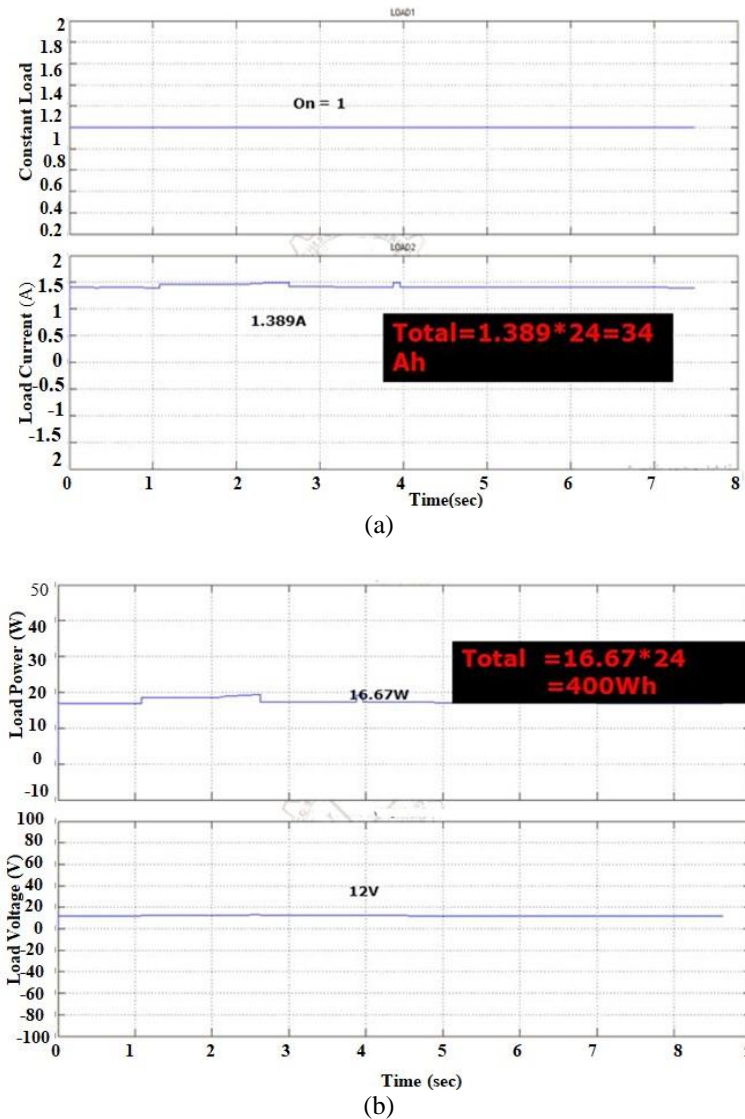

(a)

(b)
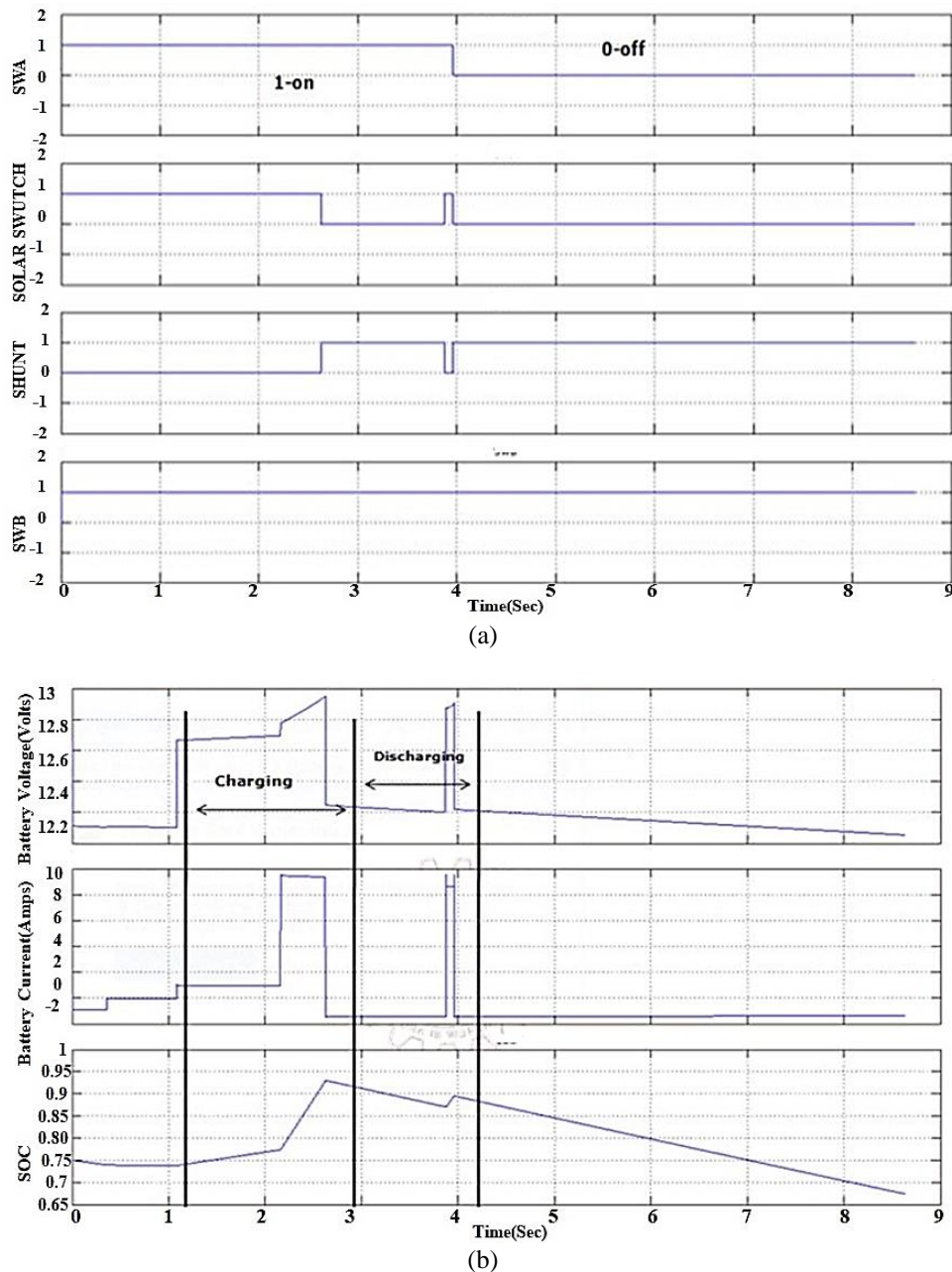
Figure 12. Switching status of SSCC and battery outptu for different insolation level or time, (a) ON and OFF status of charge controller, and (b) battery voltage, current and SOC waveforms at constant load R = 8.64Ω

(a)

(b)

Figurr 13. Load waveforms for different insolation level under constant load: (a) current and
(b) power and voltage

Table 7. Output of proposed overall standalone system for constant load under different insolation levels

Time in sec (hour)	Insolation G W/m²	PV module output (converter input)			Converter voltage	Battery Output			Charge controller (PMS switching operation)			
		V_{in} (V)	I_{in} (A)	P_{in} (W)	V_{out} (V)	V_{bat} (V)	I_{bat} (A)	SOC (%)	Solar switch (SC)	SA (Series)	Shunt (SD)	SB (Load) R = 8.64 Ω
0 (5 AM)	100	5.56	0.69	3.86	7.61	12.11	- 0.89	74.2	1	1	0	1
3600 (6 AM)	200	11.12	1.34	15.45	11.5	12.1	-0.07	73.7	1	1	0	1
10800 (9 AM)	300	16.67	2.08	34.75	14.4	12.67	0.94	77.2	1	1	0	1
21600 (12 AM)	1000	41.38	5.17	214.1	18.9	12.91	9.46	92.1	1	1	0	1
28800 (2 PM)	800	39.68	4.96	0.2	18.6	12.2	-1.41	88.1	1	0	1	1
39600 to 86400 (2 PM – 5PM)	0.01	5e-3	6.9e-05	3.8e-08	0.01	12.14	-1.39	67.7	0	0	1	1

4.2. Variable load analysis

In order to analyze the performance of the system under various loads such as pumps/motors, radios, lamps in kitchens and lounges, TV and computers. At 12V and by varying the current usage over a full day (24 hours), the loads are found to be of different values of resistances. Figure 14(a) illustrates the ON and OFF status of load based on requirement that can be powered by the PV source or the battery at predetermined times using switching strategy through charge controller. Figure 14(b) clearly shows that the switching sequence of charge controller with different insolation level for different loads under various operating times.

(a)

(b)
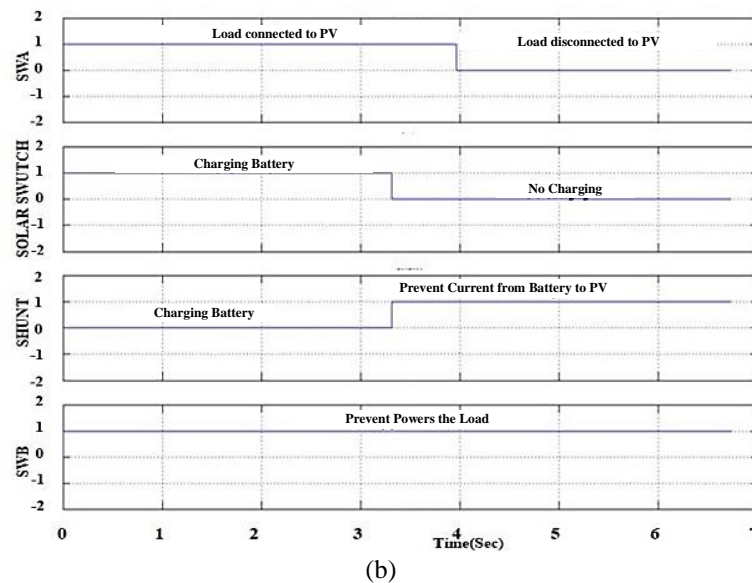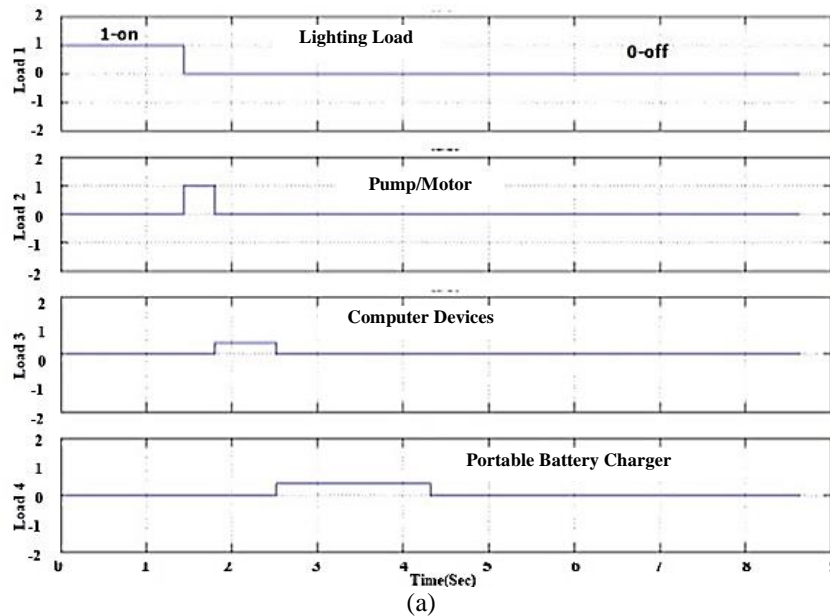
Figure 14. Switching waveforms showing the ON and OFF position of several switches for different insolation level at variable load: (a) load requirement and (b) charge controller

From the Figure 15, it is inferred that, the negative battery current clearly depicts that the battery is getting discharged during low insolation level or high loaded condition. Further the battery current is positive shows that the battery gets charged during low loaded condition or high input condition. Moreover, the battery voltage is maintained between 12.95 V and 11.6 V in all operating conditions to enhance the battery life.

Figure 16(a) clearly depicts that the voltage waveforms of different loads at their respective operating time. Figure 16(b) and Figure 16(c) clearly illustrates that the current and power consumed by

different loads fed various insolation levels in diverse operating times From the Figure 16, it was inferred that the total Ampere hour is equal to 34 Ah ((1.26 × 4) + (15.61 × 1) + (4.18 × 2) + (0.88 × 5)) = 34 Ah) and the energy consumed by the load is found to be (16.67 × 24 = 400 Wh) equal to 397 Wh/day. Table 8 clearly illustrates the output of the proposed   system for different loads under various insolation levels. From the table it is found that the switching action of SSCC based on the operating time of load.
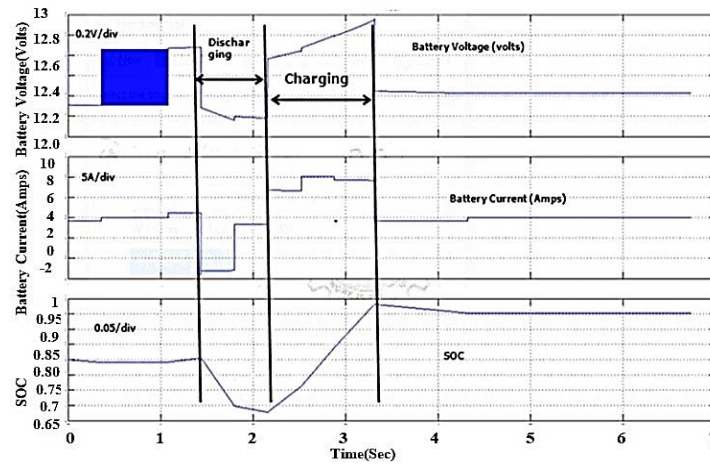
Figure 15. Output of Battery voltage, current and SOC for different insolation level at various loads
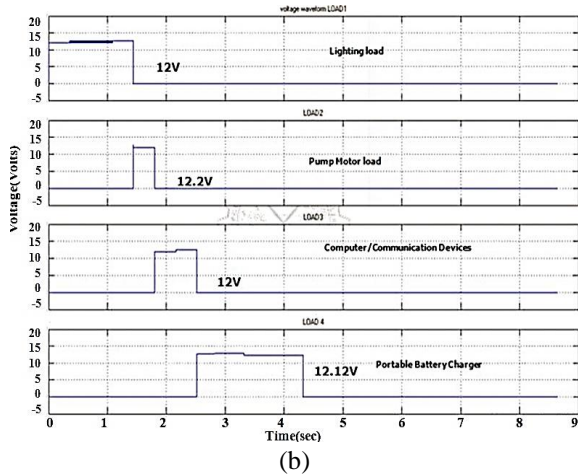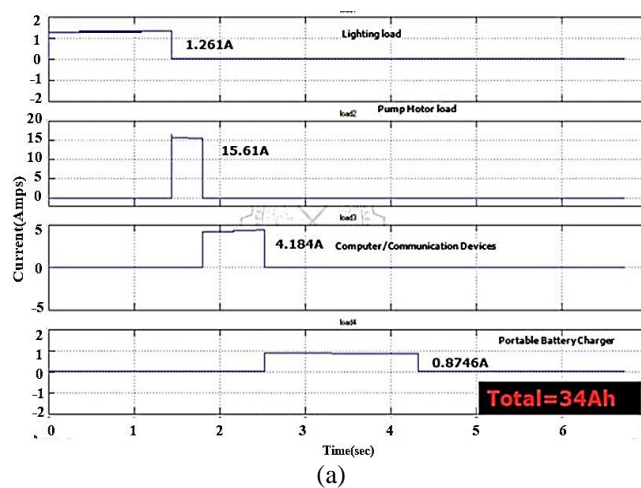

(a)

(b)

(c)
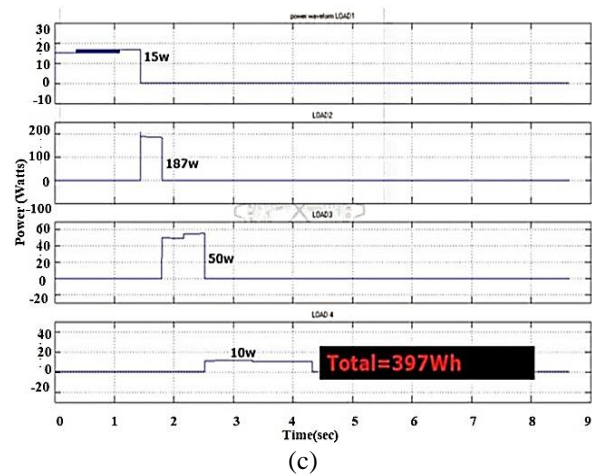
Figure 16. Load waveforms under various loaded condition for different insolation level or different operating time: (a)voltage, (b) current, and (c) power

Table 8. Output of proposed overall standalone system for various loads under different insolation levels

Time in sec (hour)	Insolation G W/m²	PV module output /converter input			Converter output	Battery output			Charge controller switching operation				Operating time period of load in hour			
		V_in (V)	I_in (A)	P_in (w)	V_out (V)	V_bat (V)	I_bat (A)	SOC (%)	Solar switch (SC)	SA (Series)	Shunt (SD)	SB	L1	L2	L3	L4
0 (5 AM)	100	5.56	0.6	3.86	7.61	12.1	-0.7	74	1	1	0	1	1 (4)			
3600 (6 AM)	200	11.12	1.3	15.4	11.5	12.1	0.07	74.1	1	1	0	1		1 (1)		
10800 (9 AM)	300	16.67	2.0	34.7	14.4	11.9	-1.6	58.6	1	1	0	1			1(2)	
21600 (12 AM)	1000	41.38	5.1	214	18.7	12.2	-0.8	91.9	1	0	1	1				1 (5)
28800 to 86400 (12AM – 5 AM)	0.01	0.01	6.9e-05	3.8e-08	1e-3	12.3	-1e-3	90.2	0	0	1	1	(12-24) hour (no load)			

Table 9. Comparison of output of proposed overall standalone system for constant and variable loads under different insolation levels

Time in sec (hour)	Insolation W/m²	Battery output					
		For constant load			For variable load		
		V_bat (V)	I_bat (A)	SOC (%)	V_bat (V)	I_bat (A)	SOC (%)
0 (5 AM)	100	12.11	- 0.89	74.2	12.1	-0.7	74
3600 (6 AM)	200	12.1	-0.07	73.7	12.1	0.07	74.1
10800 (9 AM)	300	12.67	0.94	77.2	11.9	-1.6	58.6
21600 (12 AM)	1000	12.91	9.46	92.1	12.2	-0.8	91.9
28800 (2 PM)	800	12.2	-1.41	88.1	12.3	-0.006	90.2
39600 to 86400 (5 PM – 2PM)	0.01	12.14	-1.39	67.7	12.2	-1.41	88.1

The performance of the entire standalone system under various input levels is compared by feeding constant and varying loads from the proposed converter with battery as a storage element. From the table 9, it is clearly illustrating that the proposed SSCC system shows a maximum state of charge of at 12 AM for both cases of loads. However, the SOC is high in constant load than varying load. Thus, the proposed SSPVG system provides much better feasible and also gives a very good economical solution for rural areas.

5. CONCLUSION

In this work, the control strategy of the proposed system is done by two elements i.e. ANFIS MPPT control logic with DC–DC BB converter and PMS with SSCC as a battery charger (BC) for voltage regulation as well as to fulfill the load demand. The proposed PMS with SSCC has been demonstrated using logical electronic switching strategy under both constant and various loads for various insolation levels. The performance of SSPVG with BC associated with DC–DC converter are analyzed using MATLAB model and the corresponding waveforms of various parameters of all the components in the proposed system are observed under different operating conditions. From the simulation results obtained, the proposed SSPVG with battery charger using logical electronic switch control has the capability of delivering the regulated voltage of 12V and power from the converter with greater efficiency. The entire system performance is also compared under various input levels by feeding constant and varying loads. The outcome clearly illustrates that the proposed SSCC system shows a maximum state of charge at 12 AM for both cases of loads. However, the SOC is high in constant load than varying load. By including BC, the power output from the converter can be utilized perfectly according to the load requirement without wasting the generating power and influence to reduce the sizing of hybrid system. Thus, the proposed SSPVG system provides feasible and a very good economical solution for rural areas under all aspects mainly, the lifespan of the battery can be

extended by using this scheme. However, the same proposed battery charger can be utilized effectively in any increased capacity of PV system in order to satisfy the load demand in future. The proposed system can be used in various applications such as self-powered system like residential loads, industrial loads, street lighting system and airport.

REFERENCES

[1]   R. J. Best, D. John Morrow, David J. McGowan, and Peter A. Crossley, "Synchronous islanded operation of a diesel generator," *IEEE Trans. on Power Syst.*, vol. 22, no. 4, pp. 2170–2176, 2007, doi:10.1109/TPWRS.2007.907449.
[2]   C.-W. Shyu, "Ensuring access to electricity and minimum basic electricity needs as a goal for the post-MDG development agenda," *Energy Sustain. Dev.*, vol. 19, pp. 29-38, 2014, doi: 10.1016/j.esd.2013.11.005.
[3]   A. Q. Al-Shetwi, M. Z.Sujod, A. Al Tarabsheh, and I. A. Altawil,"Design and economic evaluation of electrification of small villages in rural area in Yemen using stand-alone PV system," *Int. J. Renew. Energy Res. IJRER*, vol. 6, no. 1, pp. 289–298, 2016.
[4]   M. M. Rahman, A. S. Islam, S. Salehin, and M. A. Al-Matin, "Development of a model for techno-economic assessment of a stand-alone off-grid solar photovoltaic system in Bangladesh," *Int. J. Renew. Energy Res. IJRER*, vol. 6, no. 1, pp. 140–149, 2016.
[5]   S. Rehman and L. M. Al-Hadhrami, "Study of a solar PV–diesel–battery hybrid power system for a remotely located population near Rafha, Saudi Arabia," *Energy*, vol. 35, pp. 4986–4995, 2010, doi:10.1016/j.energy.2010.08.025.
[6]   A.M.O. Haruni, M.Negnevitsky, Md E. Haque and A.Gargoom, "A novel operation and control strategy for a standalone hybrid renewable power system," *IEEE Transactions on Sustainable Energy*, vol. 4, no. 2, pp. 977–685, 2013, doi: 10.1109/TSTE.2012.2225455.
[7]   N. Mezzai, D. Rekioua, T. Rekioua, A. Mohammedi, K. Idjdarane, and S. Bacha, "Modeling of hybrid photovoltaic/wind/fuel cells power system," *Int. J. Hydrogen Energy*, vol. 39, pp. 15158–15168, 2014, doi: 10.1016/j.ijhydene.2014.06.015.
[8]   K. Ding, X.G. Bian, H.H. Liu, and T. Peng, "A MATLAB-simulink-based PV module model and its application under conditions of nonuniform irradiance," *IEEE Trans. on Ener. Conv*, vol. 27, pp. 864–872, Dec. 2012, doi:10.1109/TEC.2012.2216529.
[9]   T. P. Sahu, T.V. Dixit and R. Kumar, "Simulation and analysis of perturb and observe MPPT algorithm for PV array using cuk converter," *Advance in Electronic and Electric Engineering*, vol. 4, no. 2, pp. 213–224, 2014.
[10]   Shanthi and A.S. Vanmukhil, "Photovoltaic generation system with MPPT control using ANFIS," *International Electrical Engineering Journal (IEEJ)*, vol. 4, no. 3, pp. 1105–1115, 2013.
[11]   S. A. Rizzo and G. Scelba. "ANN based MPPT method for rapidly variable shading conditions," *Applied Energy*, vol. 145, pp. 124–132, 2015, doi: 10.1016/j.apenergy.2015.01.077.
[12]   A. Safari and S. Mekhilef, "Simulation and hardware implementation of incremental conductance MPPT with direct control method using cuk converter," *IEEE Trans. on Indus.Electr.*, vol. 58, pp. 1154–1161, April 2011, doi: 10.1109/TIE.2010.2048834.
[13]   S. Alagammal and N. Rathina Prabha, "Investigation of performance of standalone solar PV system with KY – SR buck boost converter using FL based direct MPPT control method," *Journal of Electrical Engineering*, vol. 18, no. 3, pp. 1–12, 2018.
[14]   S. Alagammal, N. Rathina Prabha and I. Aarthy, "Centralized solar PV systems for static loads using constant voltage control method," *Circuits and systems*, vol. 7, no.10, pp. 4213–4226, 2016, doi: 10.4236/cs.2016.713346.
[15]   J. PrasanthRam, T. Sudhakar Babu, and N. Rajasekar, "A comprehensive review on solar PV maximum power point tracking techniques," *Renewable and Sustainable Energy Reviews*, vol. 67, pp. 826–847, 2017, doi: 10.1016/j.rser.2016.09.076.
[16]   S. M. Mousavi G. and M. Nikdel, "Various battery models for various simulation studies and applications," *Renewable and Sustainable Energy Reviews*, vol. 32, pp. 477–485, Apr. 2014, doi: 10.1016/j.rser.2014.01.048.
[17]   S. D. G. Jayasinghe, D. M. Vilathgamuwa, and U. K. Madawala, "Direct integration of battery energy storage systems in distributed power generation," *IEEE Transactions on Energy Conversions*, vol. 26, no. 2, pp. 977–685, 2011, doi: 10.1109/TEC.2011.2122262.
[18]   D. Fendri, and M. Chaabene, "Dynamic model to follow the state of charge of a lead-acid battery connected to photovoltaic panel," *Energy Conversion and Management,* vol. 64, pp.587–593, 2012, doi: 10.1016/j.enconman.2012.05.027.
[19]   M. M. Iqbal, and K. Islam, "Design and simulation of a PV System with battery storage using bidirectional DC-DC converter using Matlab Simulink," *International Journal of Scientific & Technology Research,* vol. 6, no. 07, pp. 403–410, July 2017.
[20]   S. Alagammal and N.R. Prabha, "Combination of modified P&O with power management circuit to exploit reliable power from autonomous PV-battery systems," *Iranian Journal of Science and Technology – Transactions of Electrical Engineering*, vol. 45, pp. 97–114, 2021, doi: 10.1007/s40998-020-00346-0.
[21]   Z. Yanhui, S. Wenji, L. Shili, L. Jie, and F. Ziping, "A critical review on state of charge of batteries," *Journal of Renewable Sustainable Energy*, vol. 5, 2013, doi: 10.1063/1.4798430.
[22]   R. Pode, "Battery charging stations for home lighting in Mekong region countries," *Renew. Sustain. Energy Rev.*, vol. 44, pp. 543–560, 2015, doi: 10.1016/j.rser.2015.01.003.
[23]   Md. Ashiquzzaman, N Afroze, Md. J Hossain, U Zobayer, and Md. Mottaleb Hossain, "Cost effective solar charge controller using microcontroller," *Canadian Journal on Electrical and Electronics Engineering* vol. 2, no. 12, pp. 571–576, 2011.
[24]   A.A. Hussein, Abbas A.A. Fardoun, "Design considerations and performance evaluation of outdoor PV battery chargers," *Renewable Energy*, vol. 82, pp. 85–91, 2015, doi: 10.1016/j.renene.2014.08.063.
[25]   T. Kamal, S. Z. Hassan, H. Li, S. Mumtaz, and L. Khan, "Energy management and control of grid-connected wind/fuel cell/battery Hybrid Renewable Energy System," *International Conference on Intelligent Systems Engineering (ICISE)*, pp. 161–166, 2016.

BIOGRAPHIES OF AUTHORS

Subbaraman Alagammal 🆔 ⑧ SC ⟳ graduated in Electrical and Electronics Engineering from Thiagarajar College of Engineering, Madurai, Tamil Nadu, India, in 1995. In 2008, she received Master of Engineering (M.E) in Power Electronics and Drives from College of Engineering, Guindy, Anna University (AU), Chennai, India. She had 8 years of teaching experience in Adhiparasakthi Engineering College, Melmaruvathur. From 2009 to 2015, she was an Assistant Professor (AP) in Electrical Engineering Department at Mepco Schlenk Engineering, Sivakasi, Tamil Nadu, India. Since 2016, she has been an AP (Sr. grade) in the same college. Now, she is pursuing her research in power electronics applications in solar energy. Her research interests are applications of power electronics converters in PV systems, MPPT controller using artificial intelligence techniques. She can be contacted at email: mshanthilogesh@mepcoeng.ac.in.

Ramachandran Bhavani 🆔 ⑧ SC ⟳ graduated in Electrical and Electronics Engineering from Thiagarajar College of Engineering, Madurai, Tamil Nadu, India, in 2000. In 2005, she received Master of Engineering (M.E) degree in Power Systems Engineering from the same college. She had 3 years of teaching experience in PSNA College of Engineering and Technology, Dindigul. From 2009 to 2015, she was an assistant professor in the Department of Electrical Engineering at Mepco Schlenk Engineering, Sivakasi, Tamil Nadu, India. Since 2016, she has been as an Assistant Professor (Sr. grade) in the same college. Now, she is pursuing her research in the field of power quality (PQ) under Anna University, Chennai, India. Her research activities are focused on analysis of PQ problems and applications of custom power devices for PQ enhancement using artificial intelligence techniques. She can be contacted at email: bavanir@mepcoeng.ac.in.

Mohammed Muhaidheen 🆔 ⑧ SC ⟳ he is working as an Associate Professor in Mepco Schlenk Engineering College, Sivakasi, India. He completed his diploma and Bachelor's degree in EEE from DOTE and Anna university, Chennai in 2003 and 2007 respectively and obtained his Master's degree in Power Electronics and Drives from Anna university, Chennai in 2003 in 2008. He completed his Doctoral degree from Anna university, Chennai in 2019. His research interests include power quality, power converter, fuzzy control, LabVIEW, inverter and internet of things. He has published several research papers in various International Journals. He is a member of various professional bodies. He can be contacted at email: muhai@mepcoeng.ac.in.